

Effects of Shear Rate on Propagation of Blood Clotting Determined Using Microfluidics and Numerical Simulations

Matthew K. Runyon,[†] Christian J. Kastrup,[†] Bethany L. Johnson-Kerner,[†]
Thuong G. Van Ha,[‡] and Rustem F. Ismagilov^{*†}

Department of Chemistry and Institute for Biophysical Dynamics, The University of Chicago,
929 East 57th Street, Chicago, Illinois 60637, and Department of Radiology, The University of
Chicago Hospitals, 5841 South Maryland Avenue, MC 2026, Chicago, Illinois 60637

Received August 21, 2007; E-mail: r-ismagilov@uchicago.edu

Abstract: This paper describes microfluidic experiments with human blood plasma and numerical simulations to determine the role of fluid flow in the regulation of propagation of blood clotting. We demonstrate that propagation of clotting can be regulated by different mechanisms depending on the volume-to-surface ratio of a channel. In small channels, propagation of clotting can be prevented by surface-bound inhibitors of clotting present on vessel walls. In large channels, where surface-bound inhibitors are ineffective, propagation of clotting can be prevented by a shear rate above a threshold value, in agreement with predictions of a simple reaction–diffusion mechanism. We also demonstrate that propagation of clotting in a channel with a large volume-to-surface ratio and a shear rate below a threshold shear rate can be slowed by decreasing the production of thrombin, an activator of clotting. These *in vitro* results make two predictions, which should be experimentally tested *in vivo*. First, propagation of clotting from superficial veins to deep veins may be regulated by shear rate, which might explain the correlation between superficial thrombosis and the development of deep vein thrombosis (DVT). Second, nontoxic thrombin inhibitors with high binding affinities could be locally administered to prevent recurrent thrombosis after a clot has been removed. In addition, these results demonstrate the utility of simplified mechanisms and microfluidics for generating and testing predictions about the dynamics of complex biochemical networks.

Introduction

This paper describes microfluidic experiments and numerical simulations to investigate the role of fluid flow in the regulation of propagation of blood clotting. Hemostasis is the complex biochemical network of ~80 reactions that control blood clotting processes, including both initiation and propagation of clotting. These reactions are regulated by many important parameters, including fluid flow, surface chemistry, and vessel geometry. The effects of fluid flow on blood clotting are of significant physiological and medical relevance. This parameter is identified as one of the three factors thought to contribute to venous and arterial thrombosis according to the classic Virchow's triad.¹ Therefore, understanding how fluid flow regulates the spatiotemporal dynamics of clotting² processes is important for treatment and prevention of cardiovascular diseases such as deep vein thrombosis³ and recurrent thrombosis.⁴ In addition, understanding this dynamics may help determine how drugs should be administered⁵ to prevent unwanted clot spreading, such as propagation of clotting into venous valves after surgery.⁴

The role of fluid flow in the regulation of clotting has been investigated extensively. However, the majority of these studies focused on initiation of clotting⁶ and platelet activation,⁷ rather than propagation of clotting. Experiments designed to study propagation of clotting have ranged from *in vivo* experiments to simplified *in vitro* experiments. While *in vivo* studies of propagation of clotting incorporate all of the relevant parameters of the network,^{8,9} experimentally controlling these parameters *in vivo* is difficult. On the other hand, simple *in vitro* studies^{10,11} that are performed under homogeneous conditions in the absence of flow allow experimental control over the biochemistry of the network but may miss the effects of fluid flow, surface

[†] The University of Chicago.

[‡] The University of Chicago Hospitals.

- (1) Cotran, R. S.; Kumar, V.; Collins, T. *Robbins Pathological Basis of Disease*, 6th ed.; W. B. Saunders Company: New York, 1999.
- (2) Kastrup, C. J.; Runyon, M. K.; Lucchetta, E. M.; Price, J. M.; Ismagilov, R. F. *Acc. Chem. Res.* **2007**, in press.
- (3) Leon, L.; Giannoukas, A. D.; Dodd, D.; Chan, P.; Labropoulos, N. *Eur. J. Vasc. Endovasc. Surg.* **2005**, *29*, 10–17.
- (4) Kearon, C. *Circulation* **2003**, *107*, 122–130.

- (5) Scott, N. A.; Nunes, G. L.; King, S. B.; Harker, L. A.; Hanson, S. R. *Circulation* **1994**, *90*, 1951–1955.
- (6) (a) Kuharsky, A. L.; Fogelson, A. L. *Biophys. J.* **2001**, *80*, 1050–1074. (b) Lo, K.; Denney, W. S.; Diamond, S. L. *Pathophysiol. Haemost. Thromb.* **2005**, *34*, 80–90. (c) Nemerson, Y.; Turitto, V. T. *Thromb. Haemost.* **1991**, *66*, 272–276. (d) Beltrami, E.; Jesty, J. *Proc. Natl. Acad. Sci. U.S.A.* **1995**, *92*, 8744–8748.
- (7) (a) Pivkin, I. V.; Richardson, P. D.; Karniadakis, G. *Proc. Natl. Acad. Sci. U.S.A.* **2006**, *103*, 17164–17169. (b) Goto, S.; Salomon, D. R.; Ikeda, Y.; Ruggeri, Z. M. *J. Biol. Chem.* **1995**, *270*, 23352–23361.
- (8) Falati, S.; Gross, P.; Merrill-Skoloff, G.; Furie, B. C.; Furie, B. *Nat. Med.* **2002**, *8*, 1175–1180.
- (9) Dorffler-Melly, J.; de Kruif, M.; Schwarte, L. A.; Franco, R. F.; Florquin, S.; Spek, C. A.; Ince, C.; Reitsma, P. H.; ten Cate, H. *Basic Res. Cardiol.* **2003**, *98*, 347–352.
- (10) Pantelev, M. A.; Ovanesov, M. V.; Kireev, D. A.; Shibeko, A. M.; Sinauridze, E. I.; Ananyeva, N. M.; Butylin, A. A.; Saenko, E. L.; Ataulakhov, F. I. *Biophys. J.* **2006**, *90*, 1489–1500.
- (11) Krasotkina, Y. V.; Sinauridze, E. I.; Ataulakhov, F. I. *Biochim. Biophys. Acta-Gen. Subj.* **2000**, *1474*, 337–345.

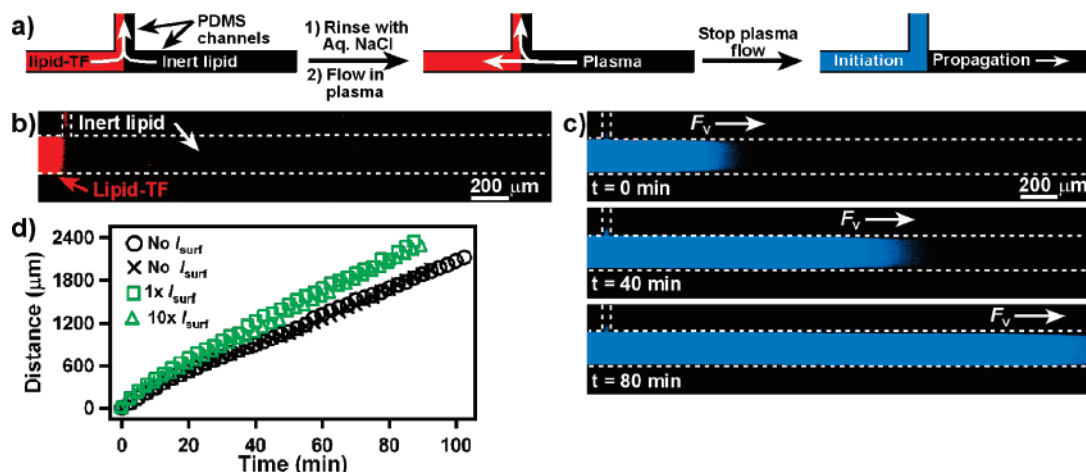


Figure 1. Characterizing propagation of blood clotting in a microfluidic channel in the absence of flow. Clots propagate with a similar front velocity, F_v , in the absence and presence of a surface-bound inhibitor of clotting, thrombomodulin (TM). (a) Schematic drawing of the procedure for initiating and monitoring propagation of clotting in a microfluidic device. Clotting (blue) initiated only on the channel walls coated with lipid-TF (red), not on the inert lipid (black), and propagated into the section of the device where inert lipids coated the channel walls. (b) A fluorescence microphotograph of a microfluidic device shows that lipids with reconstituted TF (lipid-TF, red) can be localized to a specific section of a channel in a background of inert lipids (black). (c) Time-lapse fluorescence microphotographs show the position of the clot (blue) at 0, 40, and 80 min after plasma was introduced into the channel. The blue fluorescence in the small outlet channel is difficult to see because the channel height is 10 times less than that of the main channel where propagation was monitored. (d) Experiments quantifying the velocity of propagation of clotting in the absence of TM (black circles and crosses, $F_v \approx 20 \mu\text{m min}^{-1}$) and in the presence of TM (green squares, lipid:TM = 7.6×10^4 , $F_v \approx 25 \mu\text{m min}^{-1}$) and green triangles, lipid:TM = 7.6×10^3 , $F_v \approx 24 \mu\text{m min}^{-1}$) in a channel with a large volume-to-surface ratio of $\sim 50 \mu\text{m}$ (see Supporting Information).

chemistry, and vessel geometry. *In vitro* microfluidic experiments that use human blood plasma are an attractive compromise, because they incorporate the biochemistry of the network while enabling control of fluid flow, surface chemistry,¹² and geometry.¹³

We have previously¹⁴ used microfluidics and human blood plasma to test a proposed mechanism for the regulation of propagation of clotting. According to this simple reaction-diffusion mechanism,^{15–17} a clot will continue to propagate if the concentration of activator, $[C_{\text{act}}]$, remains above some critical concentration, $[C_{\text{crit}}]$, and clot propagation will stop if $[C_{\text{act}}]$ falls below $[C_{\text{crit}}]$. Based on this mechanism, we predicted and experimentally confirmed¹⁴ that a clot will propagate as a reactive front and that this front will stop at a junction between two channels if the shear rate, $\dot{\gamma}$ [s^{-1}], in the channel with flow is above some threshold shear rate, $\dot{\gamma}_{\text{thresh}}$.

Here, we used microfluidic experiments and numerical simulations to investigate how and when shear rate regulates propagation of clotting. These results demonstrate that propagation of clotting can be regulated by two different mechanisms depending on the volume-to-surface ratio of a channel. In small channels with a small volume-to-surface ratio, propagation of clotting can be prevented by surface-bound inhibitors of clotting present on channel walls. In large channels with a large volume-to-surface ratio where surface-bound inhibitors are less effective, propagation of clotting can be prevented by a shear rate above a threshold shear rate. We also demonstrate that propagation

of clotting in a channel with a large volume-to-surface ratio and a shear rate below a threshold shear rate can be slowed by decreasing the production of activators. Combined, these results show that microfluidics¹⁸ and chemical systems^{15,19} can be used to generate and test predictions about complex biochemical networks to provide insight into the dynamics of the network.

Results and Discussion

Clots propagate as a reactive front with a constant velocity. We used a previously developed microfluidic system that enabled control of flow, geometry, and surface chemistry to produce an *in vitro* representation of blood vessels. This system was fabricated in poly(dimethylsiloxane) (PDMS).²⁰ Initiation and propagation of clotting were spatially separated by patterning the walls of the same channel with different phospholipids (Figure 1a) as previously described.¹⁴ Briefly, this patterning was accomplished by flowing two laminar²¹ streams containing phospholipid vesicles into the device from opposite ends of the channel. One stream contained a mixture of lipids that initiate clotting—phosphatidylcholine, phosphatidylserine, and Texas Red phosphoethanolamine with reconstituted tissue factor²² (lipid-TF, shown in red, Figure 1a)—and the other stream contained a lipid that does not initiate clotting—egg phosphatidylcholine (Egg PC) (inert lipid, shown in black, Figure 1a). Next, the channels were rinsed with an aqueous solution of NaCl to remove excess lipid vesicles, leaving a coating of either lipid-TF or inert lipids on the channel walls (Figure 1a and 1b). Then, blood plasma was flowed into the device from the end of the channel with inert lipids and allowed

(12) Hovis, J. S.; Boxer, S. G. *Langmuir* **2001**, *17*, 3400–3405.

(13) Khademhosseini, A.; Langer, R.; Borenstein, J.; Vacanti, J. P. *Proc. Natl. Acad. Sci. U.S.A.* **2006**, *103*, 2480–2487.

(14) Runyon, M. K.; Johnson-Kerner, B. L.; Kastrup, C. J.; Van Ha, T. G.; Ismagilov, R. F. *J. Am. Chem. Soc.* **2007**, *129*, 7014–7015.

(15) Runyon, M. K.; Johnson-Kerner, B. L.; Ismagilov, R. F. *Angew. Chem., Int. Ed.* **2004**, *43*, 1531–1536.

(16) (a) Kastrup, C. J.; Runyon, M. K.; Shen, S.; Ismagilov, R. F. *Proc. Natl. Acad. Sci. U.S.A.* **2006**, *103*, 15747–15752. (b) Kastrup, C. J.; Shen, F.; Ismagilov, R. F. *Angew. Chem., Int. Ed.* **2007**, *46*, 3660–3662.

(17) (a) Kastrup, C. J.; Ismagilov, R. F. *J. Phys. Org. Chem.* **2007**, *20*, 711–715. (b) Kastrup, C. J.; Shen, F.; Runyon, M. K.; Ismagilov, R. F. *Biophys. J.* **2007**, *93*, 2969–2977.

(18) (a) McDonald, J. C.; Whitesides, G. M. *Acc. Chem. Res.* **2002**, *35*, 491–499. (b) Quake, S. R.; Scherer, A. *Science* **2000**, *290*, 1536–1540.

(19) (a) Kaminaga, A.; Vanag, V. K.; Epstein, I. R. *Angew. Chem., Int. Ed.* **2006**, *45*, 3087–3089. (b) Winfree, A. T. *Science* **1994**, *266*, 1003–1006.

(20) McDonald, J. C.; Duffy, D. C.; Anderson, J. R.; Chiu, D. T.; Wu, H. K.; Schueller, O. J. A.; Whitesides, G. M. *Electrophoresis* **2000**, *21*, 27–40.

(21) Ismagilov, R. F.; Stroock, A. D.; Kenis, P. J. A.; Whitesides, G.; Stone, H. A. *Appl. Phys. Lett.* **2000**, *76*, 2376–2378.

(22) Smith, S. A.; Morrissey, J. H. *J. Thromb. Haemost.* **2004**, *2*, 1155–1162.

to contact the lipid–TF, and the flow was stopped. Clotting was monitored by using bright-field microscopy to detect fibrin formation and fluorescence microscopy to detect thrombin-induced cleavage of a peptide-modified dye (see Supporting Information).²³

Clotting initiated only where the channel walls were coated with lipid–TF. This clot propagated into the section of the device coated with inert lipid (Figure 1a). As predicted,¹⁵ this clot propagated throughout the channel as a reactive front²⁴ with a constant front velocity, $F_v \approx 20 \mu\text{m min}^{-1}$ (Figure 1c and 1d). This observation reinforces the question “what limits the size of a clot formed?”²⁵

In channels with a small volume-to-surface ratio, a surface-bound inhibitor is sufficient to prevent propagation of clotting. Thrombomodulin (TM), a surface-bound inhibitor of clotting present on vessel walls, has been previously proposed to regulate propagation of clotting.²⁶ TM has been shown to reduce propagation of clotting when homogeneously mixed into blood plasma.¹⁰ A surface-bound inhibitor such as TM has been suggested to have the largest affect in channels with a small volume-to-surface ratio,²⁷ such as capillaries.²⁸ To test this hypothesis, we performed 3D numerical simulations in channels with small and large volume-to-surface ratios, in both the presence and absence of a surface-bound inhibitor, I_{surf} .

These simplified 3D simulations were based on previously described rate equations¹⁶ for a proposed modular mechanism for hemostasis¹⁵ and do not require a significant amount of computational power (see Supporting Information for the rate equations). In these simulations “clotting” occurs when $[C_{\text{act}}]$ exceeds $[C_{\text{crit}}]$. In simulations using these simplified equations, F_v was approximately 10 times faster than that observed experimentally. This difference may be partially explained by the fact that experiments were performed at 25 °C, and the rate constants used in the simulation were for reactions occurring at 37 °C (see Supporting Information for measurements of F_v at 37 °C). In small $10 \times 10 \mu\text{m}^2$ channels (volume-to-surface ratio = $2.5 \mu\text{m}$) in the absence of I_{surf} , “clotting” propagated with a constant front velocity, $F_v = 210 \mu\text{m min}^{-1}$ (squares, Figure 2b), and propagation was inhibited when I_{surf} was incorporated (circles, Figure 2b). However, in large $200 \times 200 \mu\text{m}^2$ channels (volume-to-surface ratio = $50 \mu\text{m}$), “clotting” propagated at a constant front velocity, $F_v = 220 \mu\text{m min}^{-1}$, (Figure 2a) in both the absence and presence of I_{surf} (crosses and triangles, Figure 2b). The volume-to-surface ratio in these square channels equals one-fourth of their cross-sectional dimension.

In channels with large volume-to-surface ratios, a surface-bound inhibitor does not affect propagation of clotting. To experimentally verify these results, we incorporated a surface-bound inhibitor of clotting, thrombomodulin (TM), at the walls of a channel with a large volume-to-surface ratio $\approx 50 \mu\text{m}$ and

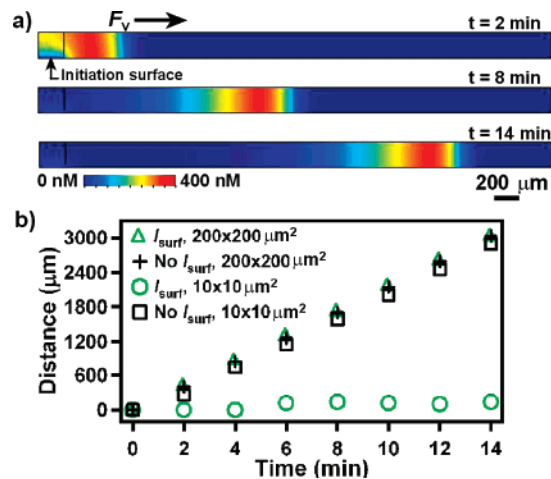


Figure 2. Propagation of “clotting” is inhibited by a surface-bound inhibitor in channels with small volume-to-surface ratios. (a) A two-dimensional projection of a three-dimensional simulation shows that the generation of activator, C_{act} , over time occurs as a reactive front with $F_v = 220 \mu\text{m min}^{-1}$. The concentration profile of C_{act} appears as a band due to inhibition of C_{act} behind the leading edge of the front. (b) Quantification of F_v in the numerical simulation in channels with small ($2.5 \mu\text{m}$, circles and squares) and large ($50 \mu\text{m}$, triangles and crosses) volume-to-surface ratios. Black crosses and squares represent simulations that do not include a surface-bound inhibitor (No I_{surf}). Green triangles and circles represent simulation conditions that include a surface-bound inhibitor (I_{surf}). See Supporting Information for details of the numerical simulation.

then experimentally quantified F_v (see Supporting Information). We incorporated TM into the inert phospholipid surface by forming inert lipid vesicles with reconstituted TM²⁹ (lipid:TM) and by using the procedure described above to coat the channel walls. Control experiments verified that TM activity on the channel walls was on the same order of magnitude as that previously measured for a monolayer of endothelial cells (see Supporting Information for experimental details and results).³⁰

When the mole ratio of lipid:TM was 7.6×10^4 , clots propagated at approximately the same velocity as without TM ($F_v \approx 25 \mu\text{m min}^{-1}$, green squares, Figure 1d). To further show that TM located at the walls of channels with these volume-to-surface ratios does not stop propagation of clotting, we increased the TM density by a factor of 10. No appreciable change in F_v was observed (green triangles, Figure 1d). Additional control experiments for both concentrations used here (Supporting Information, Table S1) demonstrated similar TM activity, and this TM activity was consistent with the saturation effects previously observed for high TM concentrations.³¹ As a control experiment, we verified that TM was sufficient to prevent propagation of clotting in small channels with a volume-to-surface ratio $\approx 5 \mu\text{m}$. In the absence of TM in these channels, clotting propagated with a constant F_v for more than 70 min. However, when 10X TM (lipid:TM = 7.6×10^3) was introduced into the inert lipids in these small channels, F_v decreased over the 70 min time interval, and the final F_v was reduced to $\sim 5 \mu\text{m min}^{-1}$. Propagation of clotting in the presence of a surface-bound inhibitor, TM, in channels with a large

(23) Kawabata, S. I.; Miura, T.; Morita, T.; Kato, H.; Fujikawa, K.; Iwanaga, S.; Takada, K.; Kimura, T.; Sakakibara, S. *Eur. J. Biochem.* **1988**, *172*, 17–25.

(24) (a) Toth, A.; Gaspar, V.; Showalter, K. *J. Phys. Chem.* **1994**, *98*, 522–531. (b) Ross, J.; Muller, S. C.; Vidal, C. *Science* **1988**, *240*, 460–465. (c) Bishop, K. J. M.; Fialkowski, M.; Grzybowski, B. A. *J. Am. Chem. Soc.* **2005**, *127*, 15943–15948.

(25) Morrissey, J. H. *J. Thromb. Haemost.* **2003**, *1*, 878–880.

(26) Esmon, C. T.; Owen, W. G. *Proc. Natl. Acad. Sci. U.S.A.* **1981**, *78*, 2249–2252.

(27) Ermakova, E. A.; Pantelev, M. A.; Shnol, E. E. *Pathophysiol. Haemost. Thromb.* **2005**, *34*, 135–142.

(28) Esmon, C. T. *J. Biol. Chem.* **1989**, *264*, 4743–4746.

(29) Feng, J.; Tseng, P. Y.; Faucher, K. M.; Orban, J. M.; Sun, X. L.; Chaikof, E. L. *Langmuir* **2002**, *18*, 9907–9913.

(30) Feistritz, C.; Schuepbach, R. A.; Mosnier, L. O.; Bush, L. A.; Di, Cera, E.; Griffin, J. H.; Riewald, M. *J. Biol. Chem.* **2006**, *281*, 20077–20084.

(31) Tseng, P. Y.; Jordan, S. W.; Sun, X. L.; Chaikof, E. L. *Biomaterials* **2006**, *27*, 2768–2775.

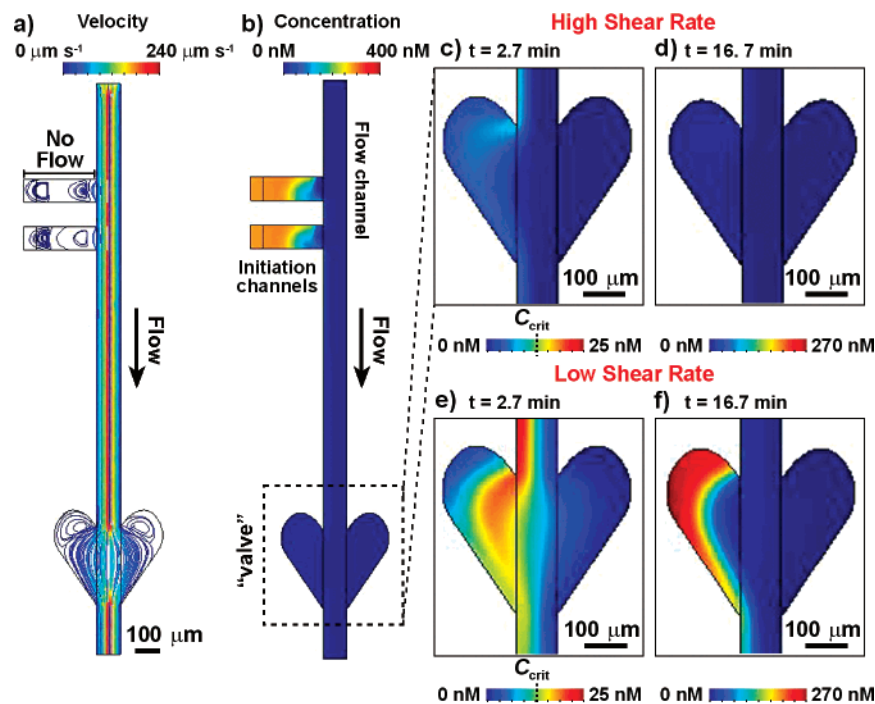


Figure 3. Propagation of “clotting” in channels with large volume-to-surface ratios is regulated by shear rate. (a) Flow profile at a shear rate of 10 s^{-1} through the geometry used in the numerical simulation. Red lines indicate streamline where the flow velocity, $V \text{ [m s}^{-1}\text{]}$, is highest, and dark blue lines indicate streamlines where V is lowest. (b) A concentration profile (scale of $0\text{--}400 \text{ nM}$) at a shear rate of 170 s^{-1} (above the threshold) shows that “clotting” does not propagate to the “valve”, because $[C_{\text{act}}]$ does not exceed $[C_{\text{crit}}]$ in the “valve”. (c) A concentration profile (scale $0\text{--}25 \text{ nM}$) of the “valve” region at the same above-threshold shear rate as in panel b shows that $[C_{\text{act}}]$ does not exceed $[C_{\text{crit}}]$. (d) A concentration profile (scale of $0\text{--}270 \text{ nM}$) of the “valve” region at the above-threshold shear rate shows that $[C_{\text{act}}]$ never exceeded $[C_{\text{crit}}]$ after the simulation reached steady state. (e) A concentration profile (scale of $0\text{--}25 \text{ nM}$) of the “valve” region at a shear rate of 10 s^{-1} (below the threshold) shows that “clotting” propagates to the “valve”, as the $[C_{\text{act}}]$ first exceeds $[C_{\text{crit}}]$ in the flow channel and then in the “valve”. (f) A concentration profile (scale of $0\text{--}270 \text{ nM}$) of the “valve” region at the same below-threshold shear rate shows that $[C_{\text{act}}]$ reaches 270 nM after the simulation reached steady state.

volume-to-surface ratio ($\sim 50 \mu\text{m}$) suggests that an additional mechanism may be responsible for regulating propagation of clotting.

In the absence of a surface-bound inhibitor, shear rate can regulate propagation of clotting in channels with a large volume-to-surface ratio. We performed numerical simulations to determine if shear rate could be an additional mechanism that regulates propagation of clotting in channels with large volume-to-surface ratios. These simulations incorporated the same device geometry as that used in previous experiments,¹⁴ including a geometry in the flow channel similar to a venous valve (“valve”). This geometry was included to reproduce the recirculating flow observed in valves (Figure 3a).³² Flow was modeled by using the Navier–Stokes equation with no-slip boundary conditions. Propagation of “clotting” was analyzed as a function of shear rate, $\dot{\gamma} \text{ [s}^{-1}\text{]}$, in the flow channel as previously described.¹⁴ The experimentally determined threshold shear rate, $\dot{\gamma}_{\text{thresh}}$, for the device geometry used in these numerical simulations and in subsequent experiments was previously determined to be $\sim 90 \text{ s}^{-1}$.¹⁴ Simulations reached steady state at $\sim 8.3 \text{ min}$ and were stopped at 16.7 min . When the shear rate in the flow channel (volume-to-surface ratio = $33 \mu\text{m}$) was above the threshold shear rate, propagation of “clotting” stopped at the junction and did not proceed to the “valve” (Figure 3b and 3c). Propagation was not observed at this above-threshold shear rate during the time course of these simulations, even after the simulations had reached steady state (Figure 3d). When the shear rate in the flow channel was below

the threshold shear rate, propagation of “clotting” continued through the junction into the “valve” (Figure 3e), eventually resulting in a high concentration of C_{act} in the “valve” after the simulation reached steady state (Figure 3f). These simulations support previous experimental results¹⁴ and demonstrated that propagation of “clotting” in a channel with a large volume-to-surface ratio can be regulated by the shear rate.

Propagation of clotting is regulated by shear rate at the junction, not at the “valve”. To test experimentally whether shear rate at the junction or at the “valve” regulates clot propagation, we designed devices that decoupled the shear rate at the junction from the shear rate at the “valve”. In the device geometry used in the numerical simulation (Figure 3) and in previous experiments,¹⁴ a change in shear rate at the junction resulted in a change in shear rate at the “valve” and, therefore, the rate of recirculation in the “valve”. Solutions were flowed into the microfluidic devices as previously described,¹⁴ and shear rates were controlled by using syringe pumps. In our experiments, a “clot time” is defined as the amount of time required for clotting to propagate from the junction to the “valve”, and a long clot time was defined as 30 min or longer. A shear rate of 190 s^{-1} (above the threshold) at both the junction and the “valve” resulted in a long clot time. However, a shear rate of 30 s^{-1} (below the threshold) at both the junction and the “valve” resulted in a short clot time. Here, when we narrowed the flow channel at the junction to generate a shear rate of 190 s^{-1} (above threshold) at the junction and a shear rate of 30 s^{-1} (below threshold) at the “valve”, a long clot time (30 min) was observed (Figure 4a), suggesting that a shear rate below the threshold at the “valve” is not sufficient to promote propagation of clotting

(32) Karino, T.; Motomiya, M. *Thromb. Res.* **1984**, *36*, 245–257.

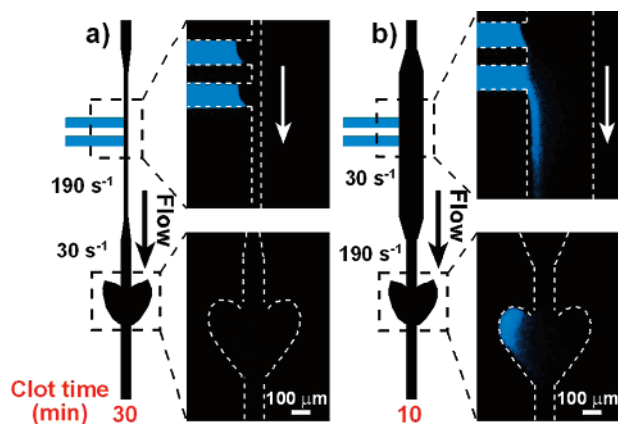


Figure 4. Propagation of clotting through a junction is regulated by shear rate at the junction and not at the “valve”. (a) Simplified schematic drawing and microphotographs at $t = 23$ min show that a shear rate above the threshold at the junction and a shear rate below the threshold at the “valve” result in a long clot time (30 min). (b) Simplified schematic drawing and microphotographs at $t = 23$ min showing that a shear rate below the threshold at the junction and a shear rate above the threshold at the “valve” result in a short clot time (10 min). Clot times are reported as the average of two experiments. In these experiments, spontaneous clotting occurred in 60–80 min. See Supporting Information Figure S2 for device dimensions and Table S2 for flow rates used in experiments.

through the junction. When we expanded the flow channel at the junction to generate a shear rate of 30 s^{-1} (below threshold) at the junction and a shear rate of 190 s^{-1} (above threshold) at the “valve”, a short clot time (10 min) was observed (Figure 4b), demonstrating that shear rate at the junction, not at the “valve”, regulates propagation of clotting.

Spreading of clotting is more rapid and extensive at below-threshold shear rates than at shear rates $\approx 0 \text{ s}^{-1}$. Above, we analyzed the conditions under which clotting would propagate from the initiation channels into the flow channel. Next, we determined the flow conditions that resulted in the most rapid and extensive spreading of clotting downstream of the initiation channels. According to a previously described mechanism,¹⁴ shear rates above the threshold will remove C_{act} fast enough to maintain $[C_{\text{act}}] < [C_{\text{crit}}]$ in the flow channel and propagation will stop at the junction. Shear rates below the threshold should transport C_{act} at concentrations greater than $[C_{\text{crit}}]$ to downstream locations in the flow channel, thus rapidly spreading the clot. However, at shear rates $\approx 0 \text{ s}^{-1}$, a clot will propagate from the initiation channels but will only spread as fast as the front velocity, F_v .

To test this hypothesis, we compared the distance that clotting spreads from the junction, d_{junct} [mm], within a set time period (27 min) at flow rates corresponding to shear rates above the threshold, below the threshold, and at shear rates corresponding to minimal flow ($\approx 0 \text{ s}^{-1}$) (Figure 5). At a shear rate above the threshold, d_{junct} was 0 mm, and the clot did not spread outside of the initiation channels (Figure 5b). When the shear rate was below the threshold, d_{junct} was 33 mm, as the flow carried a high concentration of activators downstream (Figure 5c).¹⁴ However, when the shear rate was $\sim 0 \text{ s}^{-1}$, the clot propagated through the junction, but only 1 mm into the flow channel ($d_{\text{junct}} = 1 \text{ mm}$), consistent with the value of F_v (Figure 5d). These results support previous observations showing that the generation of C_{act} is more persistent in the presence of flow than in the absence of flow.³³ Combined, these experiments show that the spreading of clots can be more severe at low shear rates than at

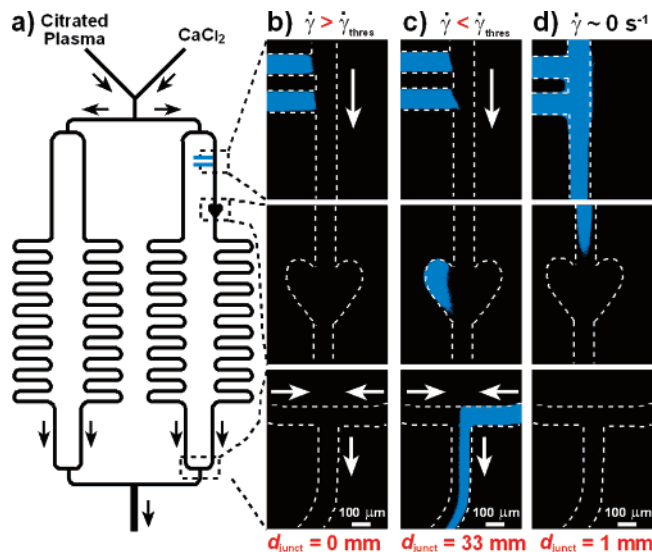


Figure 5. Clotting spreads faster in flow (at shear rates below the threshold) than in the absence of flow. (a) Simplified schematic drawing of the geometry of the device used to monitor the spread of clotting. (b) Microphotographs show that propagation of clotting stops at the junction and does not spread into the flow channel ($d_{\text{junct}} = 0 \text{ mm}$) when the shear rate is above the threshold. (c) Microphotographs show that propagation of clotting continues through the junction and spreads throughout the flow channel ($d_{\text{junct}} > 33 \text{ mm}$) when the shear rate is below the threshold. (d) Microphotographs show that propagation of clotting continues through the junction but does not spread throughout the flow channel ($d_{\text{junct}} = 1 \text{ mm}$) in the absence of flow, $\dot{\gamma} \approx 0 \text{ s}^{-1}$. The data in panels b and c were reported in ref 13 and is shown here only for comparison. Arrows indicate the direction of flow. Microphotographs shown at $t = 27$ min.

shear rates $\sim 0 \text{ s}^{-1}$. These results also suggest that a vessel in which flow at a shear rate below the threshold is stopped will occlude more rapidly than a vessel with no flow.

Propagation of clotting at below threshold shear rates can be slowed by decreasing the rate of production of activator. The proposed regulatory mechanism¹⁴ suggests that propagation of clotting stops at the junction when the rate of removal of activators exceeds the rate production of activators and maintains $[C_{\text{act}}] < [C_{\text{crit}}]$ in the flow channel. Therefore, decreasing the rate of production of activator should decrease the shear rate required to maintain $[C_{\text{act}}] < [C_{\text{crit}}]$. To test this hypothesis, we briefly exposed a clot at the junction to an irreversible direct thrombin inhibitor, D-phenylalanyl-L-prolyl-L-arginyl-chloromethyl ketone³⁴ (PPACK, Figure 6a). Thrombin was selected as the target for inhibition, because it is a potent activator of clotting that is generated in high concentrations during propagation of clotting and participates in positive feedback.³⁵ Recalcified blood plasma was flowed into the device at a shear rate greater than the threshold, and clotting was initiated as in the case of Figure 1. When the clot reached the junction, PPACK (final concentration = $0.75 \mu\text{M}$) was incorporated into the plasma and flowed in at a shear rate greater than the threshold for 7 min. To remove residual PPACK, the flow of PPACK was stopped, and recalcified blood plasma was flowed in at a shear rate greater than the threshold (see Supporting Information for experimental details). Then, the flow of recalcified blood plasma was reduced to a shear rate below the threshold, and

(33) Orfeo, T.; Butenas, S.; Brummel-Ziedins, K. E.; Mann, K. G. *J. Biol. Chem.* **2005**, *280*, 42887–42896.

(34) Kettner, C.; Shaw, E. *Thromb. Res.* **1979**, *14*, 969–973.

(35) Mann, K. G.; Brummel, K.; Butenas, S. *J. Thromb. Haemost.* **2003**, *1*, 1504–1514.

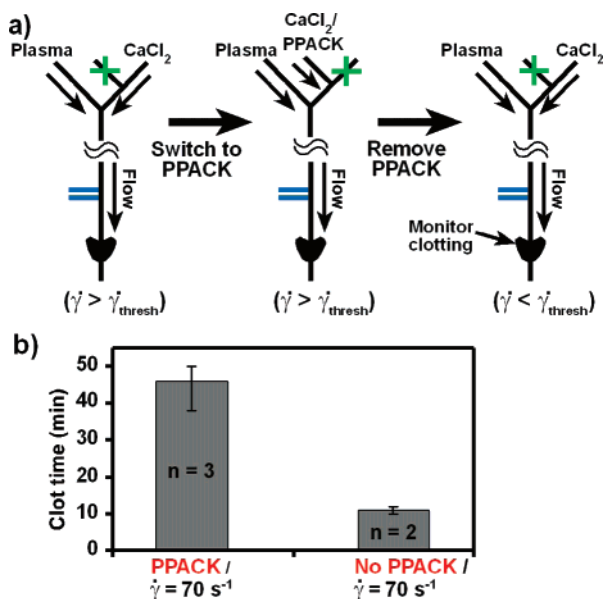


Figure 6. Propagation of clotting through a junction when shear rate in the flow channel is less than the threshold shear rate can be reduced by briefly exposing the clot at the junction (interface between blue and black channels) was exposed to PPACK. (a) Schematic drawing of an experiment in which the edge of a clot at the junction (interface between blue and black channels) was exposed to PPACK. (b) Quantification of the effect of a 7 min PPACK exposure on clot time when shear rate in the flow channel was below the threshold shear rate. Propagation of clotting was significantly reduced after a 7 min PPACK exposure. Average values are shown; error bars represent the minimum and maximum values.

propagation of clotting was monitored as in the case of Figure 1d. This 7-min PPACK exposure significantly slowed propagation of clotting into the “valve”, increasing the clot time from 11 min without PPACK exposure to 46 min with PPACK exposure (Figure 6b). Control experiments in the absence of PPACK verified that the clot at the junction remained active after a 10 min exposure to a shear rate above the threshold, as propagation of clotting resumed when the shear rate was reduced below the threshold (see Supporting Information for experimental details).

These results may appear counterintuitive—how does the clot that has been exposed to a shear rate above the threshold remain active and resume propagation as soon as the shear rate is reduced to below the threshold? In other words, how does an apparently inactive clot “reactivate” and resume propagation as is seen in cases of recurrent thrombosis? What is the molecular mechanism of this “reactivation”? One hypothesis is provided by the work on the molecular basis of memory³⁶—such a reactivation can be the result of a combination of the positive feedback loops, autocatalytic production of activators, and spatial localization of activators within the clot. Indeed, thrombin is produced autocatalytically and via a positive feedback loop³⁵ and can be localized in the active form within the clot by binding to fibrin.³⁷ We attribute the clot “reactivation” to thrombin and other clotting factors localized within the clot, and these results show that irreversible inhibition of thrombin by PPACK can prevent this “reactivation”. These *in vitro* results complement previous *in vivo* studies demonstrating that local administration of PPACK at sites of vascular damage

required concentrations of several orders of magnitude lower than in systemic administration⁵ to achieve the same antithrombotic effect. Combined, these results suggest that local delivery of irreversible direct thrombin inhibitors or reversible direct thrombin inhibitors with high binding affinities, such as hirudin³⁸ ($K_d = 25 \text{ fM}$), could effectively prevent recurrent thrombosis through the prolonged inhibition of thrombin localized in the clot.

Conclusions

Localization of clots to sites of vascular damage is a key function of the complex network of hemostasis, and understanding the dynamics of this phenomenon requires consideration of both the molecular components of the network and parameters influencing the network, including fluid flow, surface chemistry, and vessel geometry. We showed that combining a simple reaction–diffusion mechanism with current biochemical knowledge of hemostasis^{22,23,26,33,35,37,39} provides testable predictions about the network at the molecular level. By using microfluidics and human blood plasma to experimentally test these predictions, the effects of parameters like fluid flow can be analyzed. This approach is complementary to detailed simulations, which may be difficult to implement and interpret at the intuitive level, and to simple models, which may be difficult to connect to specific molecules involved.

Confirmation of these results *in vivo* is necessary, and the previously described method of intravital microscopy⁸ could be expanded to test many of these results. For example, intravital microscopy could be used to study the role of TM in the regulation of propagation of clotting in small and large vessels by using TM deficient mice⁹ or to study propagation of clotting at vessel junctions at different shear rates. Though this technique has traditionally been performed in mice,⁸ it could be expanded to studies in the microvasculature of additional model organisms such as canine and swine. For *in vivo* experiments, blood flow could be monitored by using a Doppler probe,⁹ vessel damage could be introduced with a pulse laser⁸ or FeCl_3 ,⁹ and clot formation could be monitored by using fluorescently labeled antibodies specific for TF, fibrinogen, and platelets.⁸ Determination of the dynamics of propagation of clotting *in vivo* will provide insight into when and how inhibitors of clotting, such as direct thrombin inhibitors, should be administered to treat and prevent cardiovascular diseases and minimize unwanted propagation of clotting.

If *in vivo* experiments confirm these results, five key insights would be provided into the spatiotemporal dynamics of hemostasis and its regulation: (1) the threshold response of propagation of clotting to shear rate at a junction between two vessels may play a role in localization of clotting; (2) propagation of clotting from superficial veins to deep veins^{3,40} may be regulated by shear rate, which might explain the correlation between superficial thrombosis and the development of deep vein thrombosis (DVT);^{3,40} (3) propagation of clotting at slow, below threshold flow rates may be more damaging and widely spread than propagation of clotting in the complete absence of flow; (4) nontoxic thrombin inhibitors with high binding affinities, such as hirudin,³⁹ may be locally administered⁵ to prevent

(36) Lisman, J. E.; Zhabotinsky, A. M. *Neuron* **2001**, *31*, 191–201.

(37) Liu, C. Y.; Nossel, H. L.; Kaplan, K. L. *J. Biol. Chem.* **1979**, *254*, 10421–10425.

(38) Liu, C. C.; Brustad, E.; Wenshe, L.; Schultz, P. G. *J. Am. Chem. Soc.* **2007**, *129*, 10648–10649.

(39) Stone, S. R.; Hofsteenge, J. *Biochemistry* **1986**, *25*, 4622–4628.

(40) Decousus, H.; Leizorovicz, A. *J. Thromb. Haemost.* **2005**, *3*, 1149–1151.

recurrent thrombosis after a clot has been removed; and (5) stringently regulating blood flow during surgeries may prevent unwanted propagation of clotting into venous valves, a condition that often occurs after surgery.⁴ These results may have implications for several other clotting disorders. For example, diabetics have an increased risk for high blood pressure and damage to small vessels such as capillaries,⁴¹ which includes clotting, that eventually may lead to amputation of the lower limbs.⁴² High blood pressure is treated with vasodilators,⁴¹ for example, hydralazine,⁴³ which reduce afterload and might have the unintended consequence of reducing shear rate at the site of action in the arterioles. Vasodilators that reduce the local shear rate below the threshold value may lead to further

(41) Brownlee, M. *Nature* **2001**, *414*, 813–820.

(42) Beckman, J. A.; Creager, M. A.; Libby, P. *JAMA-J. Am. Med. Assoc.* **2002**, *287*, 2570–2581.

(43) Beers, M. H.; Porter, R. S.; Jones, T. V.; Kaplan, J. L.; Berkwitz, M. *The Merck Manual of Diagnosis and Therapy*, 18 ed.; Merck Research Laboratories: Whitehouse Station, 2006.

propagation of clotting already present in diabetics and to extensive thrombosis.

Acknowledgment. This work was funded by the ONR (Grant N000140610630), the NSF CAREER Award (CHE-0349034), and the Camille Dreyfus Teacher-Scholar Awards Program. M.K.R. was supported in part by Burroughs Wellcome Fund Interfaces I.D. 1001774. R.F.I. is a Cottrell Scholar of Research Corporation and an A. P. Sloan Research Fellow. Some of this work was performed at the MRSEC microfluidic facility (funded by the NSF). We thank Jessica M. Price for contributions in writing and editing this manuscript.

Supporting Information Available: Detailed procedure for the experiments and numerical simulations. This material is available free of charge via the Internet at <http://pubs.acs.org>.

JA076301R